Star-Disk Interaction in Young Stars
Proceedings IAU Symposium No. 243, 2007
J. Bouvier & I. Appenzeller, eds.
© 2007 International Astronomical Union
DOI: 00.0000/X000000000000000X

Gas at the inner disk edge

John S. Carr [1]

[1] Naval Research Laboratory, Remote Sensing Division, Washington, DC 20375, USA
email: carr@nrl.navy.mil

Abstract. Infrared molecular spectroscopy is a key tool for the observation of gas in the innermost region of disks around T Tauri stars. In this contribution, we examine how infrared spectroscopy of CO can be used to study the inner truncation region of disks around T Tauri stars. The inferred inner gas radii for T Tauri star disks are compared to the inner dust radii of disks, to the expectations of models for disk truncation, and to the orbital distribution of short-period extra-solar planets.

Keywords. Accretion disks, protoplanetary disks, stars: formation.

1. Introduction

The star-disk interaction takes place within a region at several stellar radii from the star. In the magnetospheric accretion paradigm, the inner accretion disk is truncated by a strong stellar magnetic field, and material accretes onto the star along magnetic field lines (Königl 1991; Cameron & Campbell 1993; Shu *et al.* 1994). The disk is thought to be truncated near the corotation radius, where the Keplerian angular velocity in the disk equals the angular velocity of the star. The magnetic coupling between the star and disk, often referred to as disk locking, has been proposed as a mechanism to regulate the angular momentum of the star and explain the slow rotation of accreting T Tauri stars (Königl 1991). Shu *et al.* (1994) combine this picture of accretion and stellar angular momentum regulation with a magnetocentrifugal wind that originates at the X-point (the corotation radius) and carries away angular momentum.

Hence, the interaction of the star and disk via magnetospheric accretion is central to current ideas of accretion, mass loss, and angular momentum evolution. The observational signatures of magnetospheric accretion are plentiful (see papers in these proceedings), but the majority of these phenomena are tied to accretion onto the star, i.e., the hot gas in the accretion columns and the shocks at the stellar surface. We have little information on the interaction of the magnetosphere with the disk. In fact, something as fundamental as the inner truncation radius of the disk, which must be near the corotation radius in disk locking models, has been poorly constrained.

In this contribution, we discuss measurements of disk gas in the inner truncation region of the disk. We focus on the classical T Tauri stars (CTTS), accreting solar-mass pre-main-sequence stars in which the star-disk interaction is historically best studied. After presenting measurements of the inner gas radius based on velocity-resolved, but spatially unresolved, spectra, we compare these results to recent interferometric measurements of the dust, to the corotation radii for individual stars, and to orbital radii of extrasolar planets.

2. Gas probes of the inner disk

The useful probes of gas in the inner disk are determined by the physical conditions of the gas and dust. Within about 1 AU of the star, temperatures are expected to range

from a few 100 K to few 1000 K. Under these conditions, molecules will be abundant in the gas phase, though molecular hydrogen may be dissociated near the inner disk edge or in a hot upper disk atmosphere. The temperatures and densities are sufficient to excite many rotational and ro-vibrational levels of molecules, whose transitions occur in the near- to mid-infrared. Hence, infrared molecular spectroscopy is a prime tool for studying the inner disk gas. High spectral resolution is particularly advantageous in the ability to provide kinematic information on the gas, which can be used to probe the gas structure and conditions as a function of Keplerian velocity. Some of the key molecules that have been observed and attributed to the inner disk are CO, H_2O, OH and both infrared and UV transitions of H_2 (see Najita *et al.* 2007 for an overview).

The infrared transitions of these molecules are normally observed in emission in CTTS. Emission lines can arise from disks under two broad scenarios. In the common case for CTTS, when the disk is optically thick, emission lines can be produced in a temperature inversion in the disk atmosphere. In this situation, the spectral features only probe the atmosphere and not the entire vertical column density of the disk. Emission lines can also be formed in regions of the disk that are optically thin in the continuum. This could be the situation at particular radii due to lower opacity as a result of dust sublimation or grain growth, or the entire column density could be greatly reduced due to dynamical clearing or disk dissipation.

3. CO emission in T Tauri stars

If one wishes to study the gas at the inner edge of T Tauri star disks, then the infrared transitions of CO are the logical choice. CO is an abundant molecule in many astrophysical contexts. The high dissociation energy of CO means that it can survive to temperatures of 4000-5000 K. Hence, CO is highly likely to be present in the disk gas around CTTS down to the inner disk edge. This situation is different from that for the higher temperature and more luminous Herbig Ae/Be stars, in which the inner gaseous disk will be hot enough, at least in the innermost regions, for CO to be dissociated. The gas in the innermost part of CTTS disks will be both dense and warm (> 1000 K) enough that the near-infrared ro-vibrational transitions will be an ideal probe of the gas.

There are two different bands of CO that are observed in emission from CTTS. The first is the overtone band, $\Delta v = 2$ transitions, that are found as a series of bandheads near 2.3μm. CO overtone emission has been shown to originate from rotating disk gas in young stellar objects over a wide range in stellar mass (Najita *et al.* 2007). The emission traces gas in the 2000-4000 K range, and in low-mass young stellar objects the emission originates very close to the central star (Carr *et al.* 1993; Carr, Tokunaga & Najita 2004). However, CO overtone emission is only observed in a small fraction of CTTS, those with the highest mass accretion rates. This limits its usefulness in studying the inner disks in the general CTTS population.

In contrast, the CO fundamental ($\Delta v = 1$) transitions near 4.7μm are observed in emission in nearly all CTTS (Najita, Carr & Mathieu 2003). The larger transition probabilities (by two order of magnitude) and the lower energy of the $v = 1$ level, means that the CO fundamental can probe lower temperature and lower column density gas than the overtone. Evidently, while the conditions for CO overtone emission are rarely met in CTTS, the conditions required for CO fundamental emission are common. Hence, the CO fundamental lines are a good general tracer of gas in the inner disk of CTTS.

Examples of the CO fundamental spectrum observed in CTTS can be seen in Najita et al. (2003). The rotational transitions of the $v = 1 - 0$ band are the strongest, and the $v = 2 - 1$ lines are seen at lower strength when the S/N is sufficient. Higher vibrational

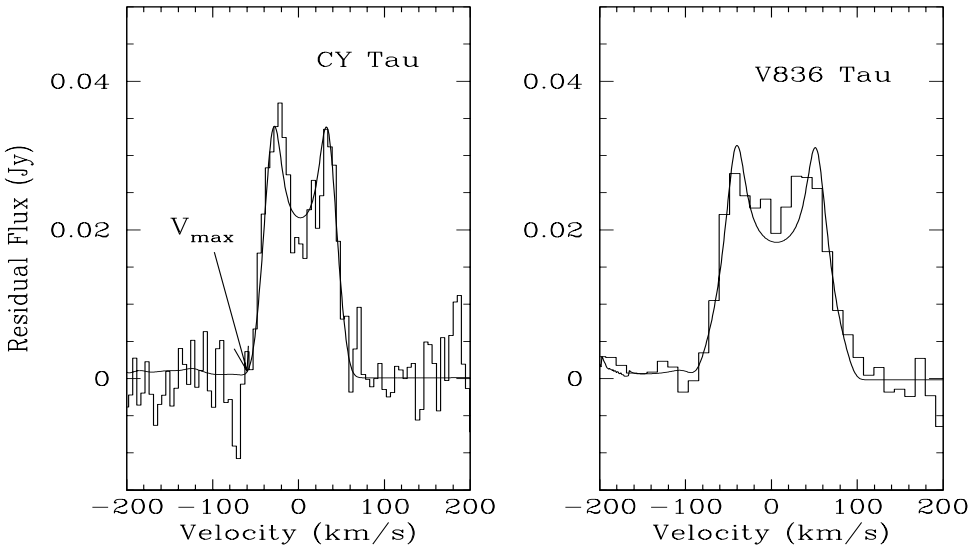

Figure 1. CO $v = 1 - 0$ line profiles for two CTTS that show a classic double-peaked disk profile (Najita, Carr & Mathieu 2003; Najita *et al.* 2007, in prep.). The smooth lines are model disk profiles. By measuring the maximum CO velocity in the profile, and knowing the stellar mass and inclination, the minimum CO gas radius follows for Keplerian rotation.

transitions (e.g., $v = 3 - 2$) and ^{13}CO $v = 1 - 0$ transitions may also be observed, depending on the gas temperature and CO optical depth. Excitation temperatures are in the general range of 500 to 1500 K. There exists a trend of stronger CO emission strength in objects with higher accretion rates (Najita, Carr & Mathieu 2003).

4. Probing gas at the inner disk edge

The disks in CTTS are expected to be truncated at distances of several stellar radii from the star, placing the region of interest inside of about 0.1 AU. This is an angular resolution of less than 1 mas at 140 pc, the distance of the Taurus star formation region. Hence, this region has not been spatially resolved until the recent advent of near-infrared interferometry (see Malbet, these proceedings). Recent work has provided the first spatially resolved information on the 2μm contiunuum in the innermost disk region (Eisner *et al.* 2005; Akeson *et al.* 2005). For study of the gas, spectro-interferometry that would allow one to spatially resolve the line emission separately from the continuum is desirable. Recent spectro-interferometry of the CO overtone bandhead emission in the Herbig Ae/Be star 15 Oph (see Malbet) illustrates the type of observations that one like to carry out for the inner gas in CTTS. However, CTTS are more challenging, given that they are much fainter and the CO emission region is expected to smaller in size. In the long term, spectro-interferometry of CO at 5μm is desirable, ideally at high spectral resolution.

Until this can be achieved, we can make progress on exploring the inner gas radii of disks by utilizing the kinematic information from line velocity profiles. For the ideal case of an emission line from a Keplerian disk, the line profile contains information on the radial variation of the gas emission. When line profiles for multiple transitions from the same molecule are included, the radial variation of gas temperature and column density can be constrained. Relative gas-phase abundances could also be derived from observations of different molecules.

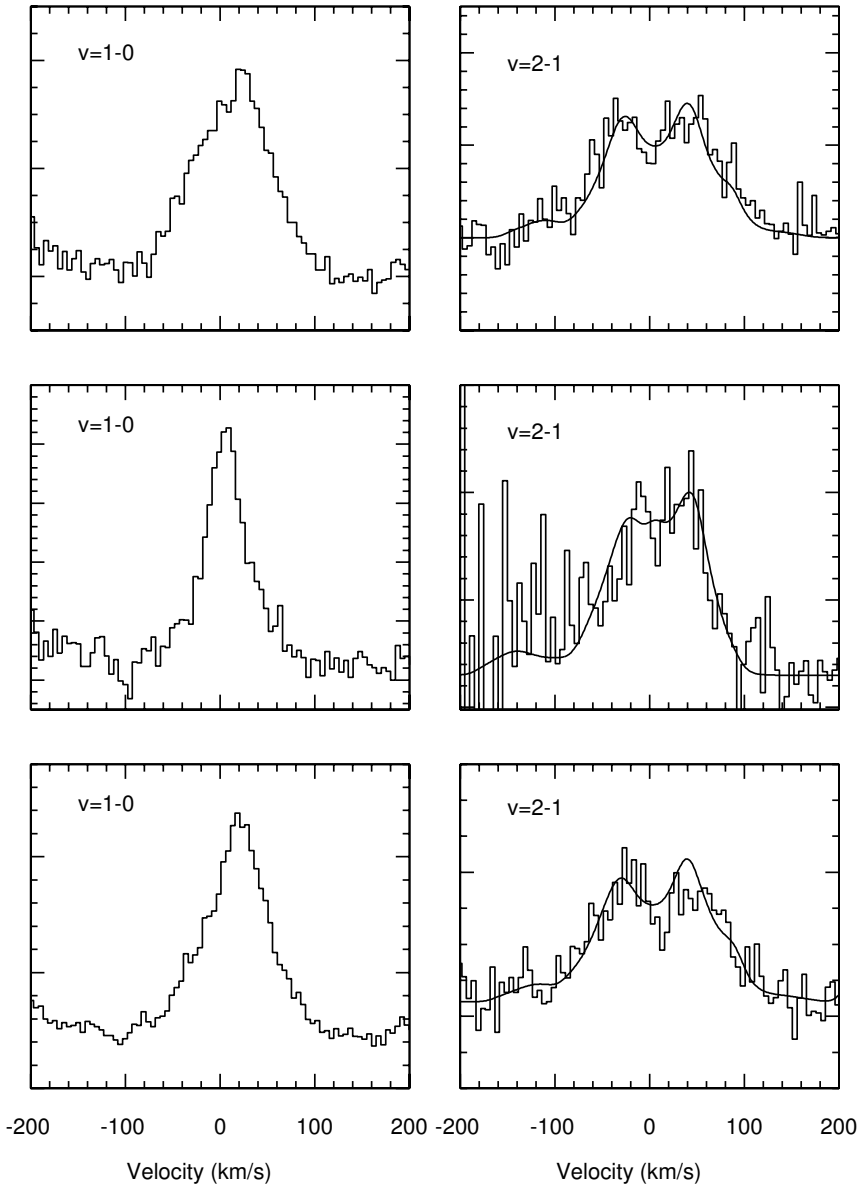

Figure 2. CO $v = 1-0$ and the $v = 2-1$ line profiles are compared for three CTTS (Carr *et al.* 2007, in prep.). The $v = 1-0$ profiles for these stars are centrally peaked, but at the same time the $v = 2-1$ profiles have a disk profile, as shown by the model disk profiles (smooth lines).

Figure 1 shows a CO $v = 1-0$ profile for two CTTS which show a classic double-peaked profile for emission from a disk. The smooth line is a model disk profile. For a Keplerian disk, the maximum observed velocity in the profile corresponds to the minimum radius at which the emission occurs. The velocity of the emission peak corresponds, roughly, to the maximum radius of the emission. Assuming that the gas is in Keplerian rotation, a

measurement of the maximum velocity gives the minimum gas emission radius, provided we know the stellar mass and the inclination. This method was first applied to CTTS profiles by Najita *et al.* (2003).

5. CO fundamental profiles

The above interpretation of the CO emission depends upon the assumption that the gas is in Keplerian rotation. While a small number of CTTS have CO $v = 1 - 0$ emission lines with the expected double-peaked profile (Fig. 1), the more common $v = 1 - 0$ profile is one that is centrally peaked, sometimes with asymmetries in the line profile (Figure 2; also see Najita *et al.* 2003 for more examples of profiles). However, when the signal-to-noise is sufficient to measure the profiles of the higher excitation $v = 2 - 1$ transitions, these tend to show a double-peaked or flat-topped profile that is consistent with emission from a disk (Figure 2). Qualitatively, more centrally peaked $v = 1-0$ lines would be expected if the $v = 1 - 0$ emission originates over a greater range of disk radii out to fairly large radii. The FWHM velocity of the $v = 2 - 1$ profiles is normally larger than the FWHM of the $v = 1 - 0$ profiles. This fits a disk scenario where the $v = 2 - 1$ lines form in hotter gas at smaller radii, and hence larger Keplerian velocities, than the bulk of the $v = 1 - 0$ emission flux. At the same time, the full-width at zero intensity of the $v = 1 - 0$ and $v = 2 - 1$ lines are similar, showing that the lines share a common maximum velocity and minimum inner disk emission radius.

The observations support the idea that the bulk of the CO fundamental emission originates from the disk. Nevertheless, some details of the profiles suggest that the picture is not the ideal case. Moderately hot gas at large radii might explain the more sharply peaked lines, and asymmetric disk emission might account for line asymmetries. Potentially, CO emission (or absorption) from either the base of the funnel flow or from the base of a molecular wind could make contributions to the profiles.

6. The inner gas radius

Measurements of the inner gas radius are presented here based on a sample of CTTS that have measurements or estimates of stellar mass and inclination and 5μm echelle spectra measured at the Keck Observatory with NIRSPEC. The data are from Najita *et al.* (2003), additional data collected by Carr, Najita and Mathieu (in prep), and one star (GM Aur) published by Salyk *et al.* (2007). The stellar mass and inclination come from one of two methods. The more robust method uses the results of Simon *et al.* (2000), who used millimeter line interferometry to image the outer disks (100 AU) around a sample of CTTS. From the disk images and the measured Keplerian velocity, they determine the central stellar mass and the disk inclination. In practice, we do not require their actual values for mass and $\sin i$, but rather their measurement of the projected velocity at 100 AU. Essentially, by knowing the projected Keplerian velocity at a known radius, the unknown radius for a different measured Keplerian velocity directly follows. In the second method, the inclination is derived from a measured stellar rotational period, $v \sin i$ for the star, and the star's radius (as determined from the stellar luminosity and temperature). The stellar mass comes from evolutionary tracks, given the stellar temperature and luminosity. This method is judged to have larger uncertainties.

For each star in the sample, the maximum CO velocity was measured from the $v = 1-0$ emission lines and used to determine the inner CO radius. Figure 3 shows the distribution of the inner gas radius as measured by CO. The distribution shows a strong peak at about 0.04 AU. In the figure, the two stars indicated by unshaded bars are systems with

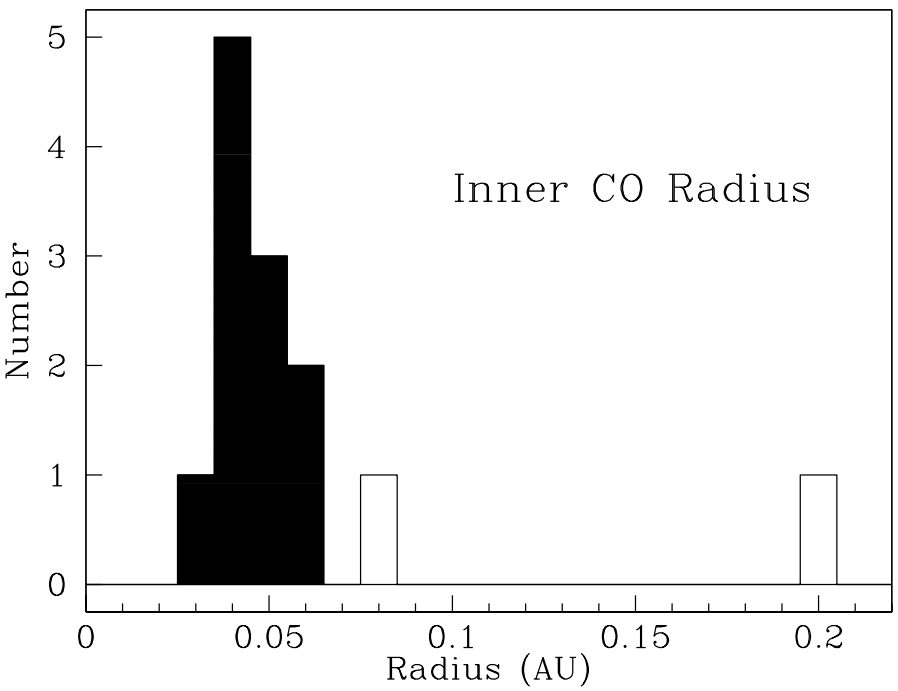

Figure 3. The distribution of inner gas radius as determined from the CO fundamental emission profiles in a sample of CTTS. The two unshaded bars are stars with transitional disks.

transitional disks, disks with large inner holes as determined from their spectral energy distributions. The inner gas radii for these systems fall at larger radii than their normal CTTS counterparts.

The inner gas radius can be compared to the co-rotation radius for each star as determined from the stellar rotational period and mass. In Figure 4, the inner gas radius is plotted vs. the co-rotation radius for the sample. The solid squares are for stars where the derived gas radii use of the results from Simon *et al.* (2000) for the stellar mass and inclination, while the open squares are for stars where the second method outlined above was used. The figure shows that the inner gas radius is typically smaller than the co-rotation radius. The average ratio of the inner gas to the co-rotation radii is about 0.7, excluding the two stars with transition disks. It is reassuring that the typical gas radius in the two group of stars, which use different methods for the mass and inclination, does not differ significantly. The error bars show the estimates of the uncertainties in the radii; the scatter in the inner gas radii appears to be consistent with the errors.

It is of major interest to compare the inner gas radius to determinations of the inner dust radius. This is shown in Figure 5. Unfortunately, the overlap in the two samples of stars is small, but the four stars in common agree with the overall comparison that dust radii are equal to or greater than the gas radii. The dust radii come from one of two techniques. The first group are inner dust radii determined from near-infrared interferometry (Eisner *et al.* 2005; Akeson *et al.* 2005). The interferometric dust radii depend on the model adopted for the geometry of the emission, usually either a flat disk or a ring, the latter being more equivalent to the inner dust rim scenario. The results for the ring or rim models are used in Figure 5. The second group of dust radii (unshaded

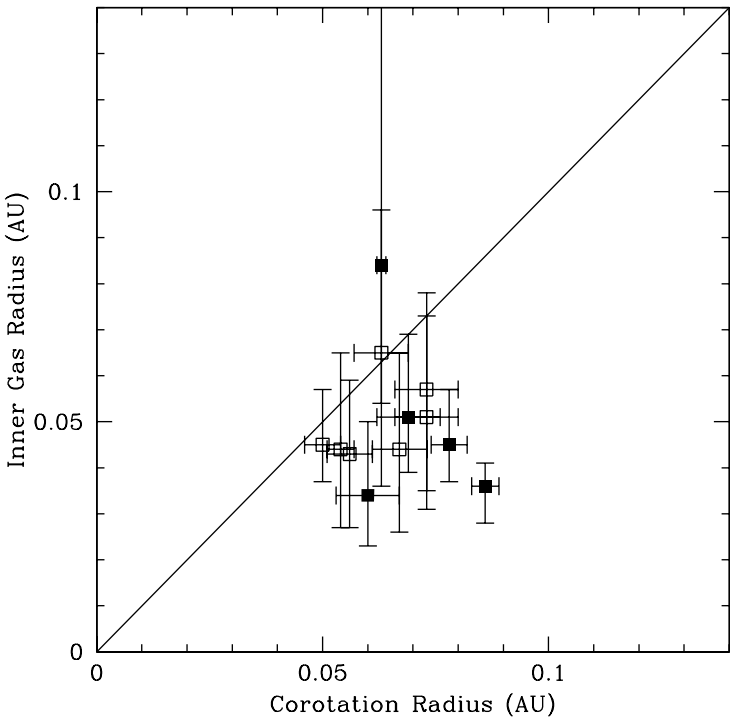

Figure 4. The inner CO gas radius plotted against the corotation radius. The solid points use the results of Simon *et al.* (2000) for determining the CO radius, while the open points use the stellar period and $v \sin i$ (see text).

histogram) are determinations of the dust inner rim radii based on modeling of the shape of the near-infrared excess continuum emission (Muzerolle *et al.* 2003).

Another way of examining the gas and dust radii is shown in Figure 6, in which the respective radii are ratioed to the co-rotation radius for each star (not all stars in the dust radius sample have a determined co-rotation radius). In contrast to the inner gas radius, the inner dust rim falls at or outside the co-rotation radius, a result that was previously noted by Muzerolle *et al.* (2003) and Eisner *et al.* (2005). Because the disk is theorized to be truncated near the corotation radius, these authors also anticipated that a gaseous disk must extend inside of the dust sublimation radius. Figures 5 and 6 show that this to indeed be the case. While this result should not be surprising, what is interesting is that the inner gas edge typically falls inside of the co-rotation radius.

Figure 7 compares the inner gas radius distribution to the distribution of orbital radii of known extrasolar planets. As has been known for some time, short-period extrasolar planets show a peak in their orbital period distribution at about 3 days. This piling up in period corresponds to an orbital radius of about 0.04 AU. As Figure 7 shows, there is an amazing coincidence in the peak of the inner gas radius distribution to the peak in planetary orbital radii. This provides strong support for the role of disk truncation in halting the inward migration of giant extrasolar planets, an idea that has been discussed in a number of papers (Lin *et al.* 1996; Kuchner & Lecar 2002; Romanova & Lovelace 2006). Note, however, that the peak in the gas inner radius is not at the outermost

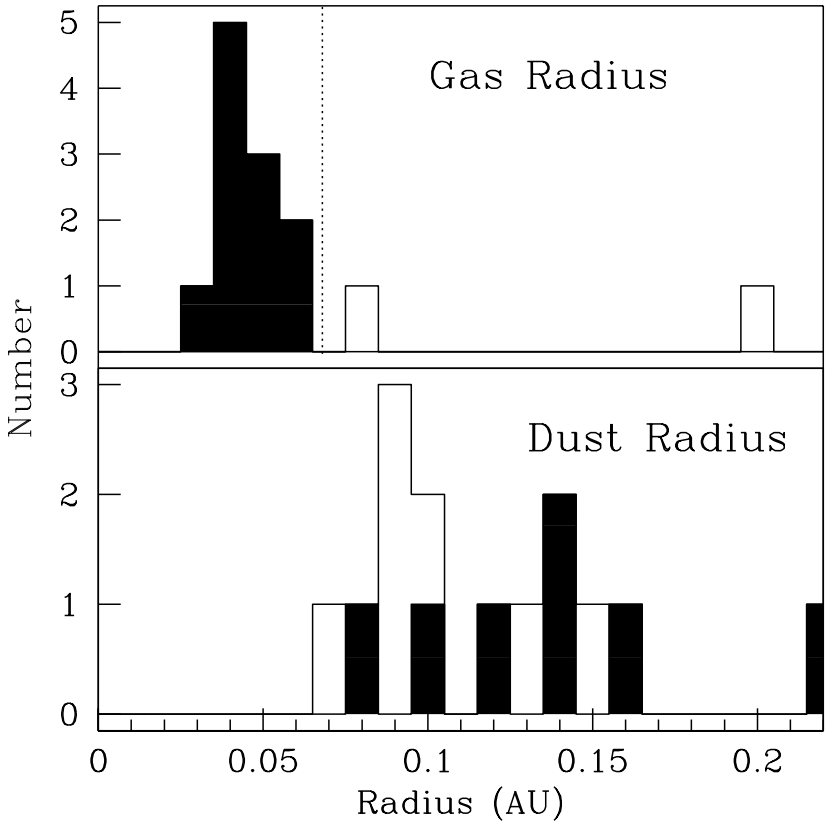

Figure 5. The distribution of inner gas radius is compared to the distribution of inner dust radius, for two different samples of CTTS. In the upper panel, symbols are the same as in Figure 4, and the vertical dotted line is the average corotation radius for the sample. In the lower panel, the shaded bars are dust radii determined from near-infrared interferometry, while the unshaded bars are from modeling the spectral energy distributions of the near-infrared excess (see text).

Lindblad resonance (1.59 times the radius) of the peak in the planetary orbit distribution, as might be expected if the CO gas radius is the physical truncation radius of the disk.

7. Discussion and summary

The results presented here for the inner gas radius as derived from spectroscopy of the CO fundamental emission in CTTS, when combined with the results for the inner dust radius, suggest a picture in which the gaseous disk extends inward of the dust sublimation radius to radii that are typically smaller than the corotation radius. In disk locking models, the magnetosphere truncates the disk near the corotation radius. To the extent that either the CO emission or near-infrared continuum emission trace the inner disk edge, it is reassuring to first order that the derived gas and dust radii are within a factor of two of the corotation radii.

For the dust, the innermost radius should be set by the dust sublimation temperature, and there is no *a priori* reason that the disk should terminate at this point. Hence, we would expect that the gas rather than the dust should be a better measure of the minimum radius of the disk.

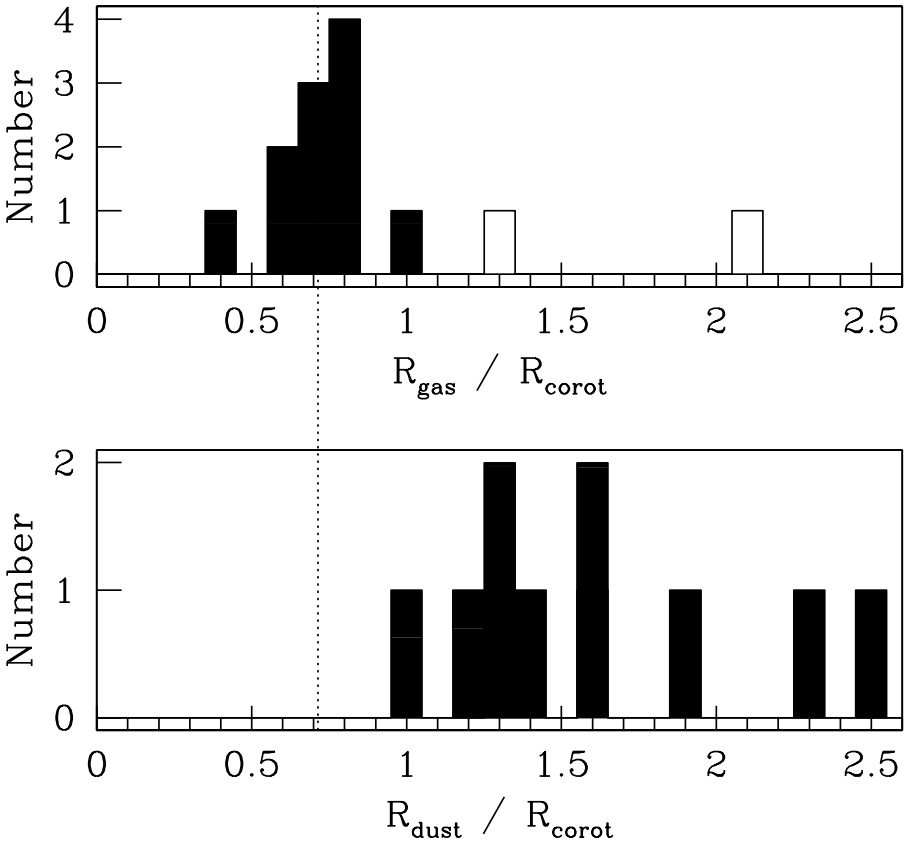

Figure 6. The distribution of inner gas and dust radii ratioed to the corotation radii are compared. The vertical dotted line is the average ratio of the gas radius to the corotation radius, equal to about 0.7. Symbols in the upper panel are the same as in Figure 4. Except for the two transitional disks, the gas radii are less than or equal to the corotation radii. The dust radii are greater or equal to the corotation radii.

How well do we know either the inner gas or dust radius? The inferred radii from near-infrared interferometry depend on the geometric model that is adopted, and results can differ by up to a factor of two in radius for a given star (Eisner *et al.* 2005; Akeson *et al.* 2005). In general, puffed-up inner rim or ring models (used in Figures 5 and 6) give better fits than a uniform flat disk, but adopting the flat or uniform disk models in Akeson *et al.* (2005) and Eisner *et al.* (2005) does not change the qualitative result that the dust radii are larger than the corotation radius.

The uncertainties for the inner CO gas radii, as shown by the error bars in Figure 4, include our best estimates of the uncertainties in the stellar parameters and the maximum CO velocity. While the errors are large enough for many stars to be consistent with the corotation radius, on average the CO emission gives a radius about 0.7 times the corotation radius. The radii that use the results of Simon *et al.* (2000) are independent of the values for mass and inclination and are not significantly different from the radii that do use mass and inclination estimates. In order to force the CO radii to agree with

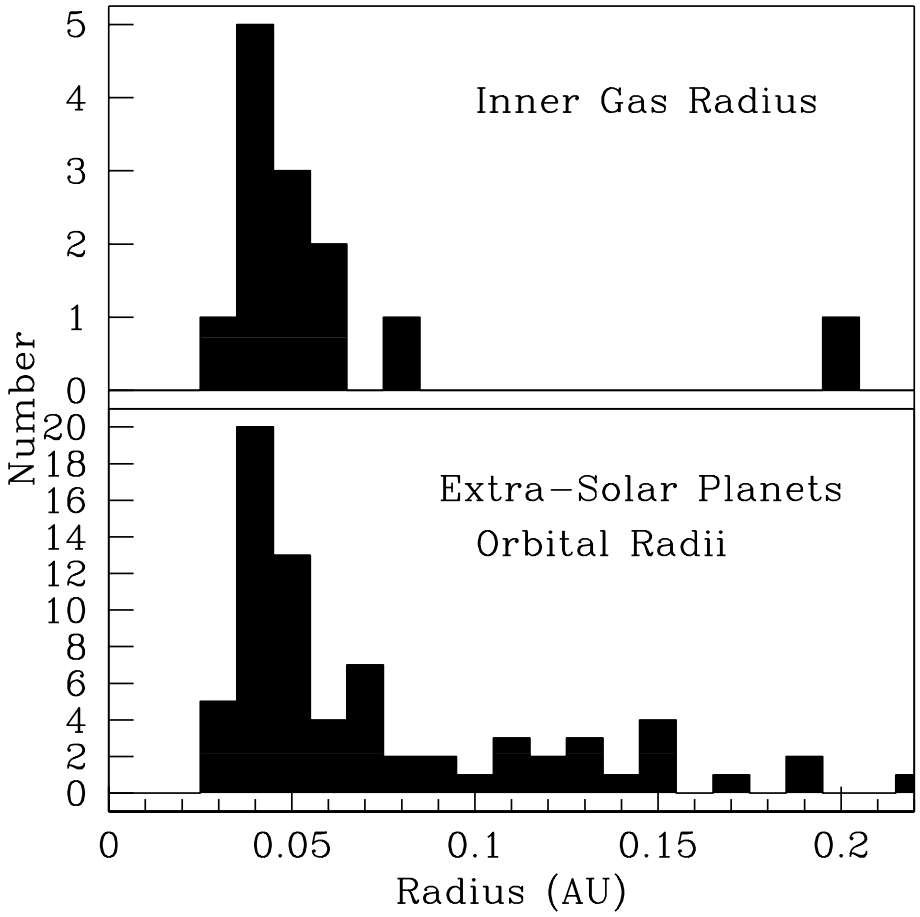

Figure 7. The distribution of inner gas radii are compared to the distribution of orbital radii for short-period extrasolar planets ("hot Jupiters"). The well known peak in the orbital radii of short-period planets coincides with the inner disk gas radius as determined from the near-infrared CO profiles.

corotation, the maximum CO velocities would have to systematically lower by a factor of 0.85, which on average is about 16 km s^{-1}. While this is excluded by the data, it is more difficult to exclude the possibility that the highest velocity in the wings of the profiles might be produced by weak emission from some kinematic component other than the disk.

An important caveat about the CO emission is that very little column density of gas is required to produce the fundamental emission. The emission observed in CTTS require total columns of $0.001 - 0.1$ g cm^{-2}, assuming all of the C is in CO. These values are order of magnitudes lower than the expected disk column densities. For example, in the disk model of D'Alessio *et al.* (1998), the column density at 0.1 AU is about 500 g cm^{-2}, for a mass accretion rate of 10^{-8} and the viscosity parameter $\alpha = 0.01$. In the general CTTS case, the CO emission is believed to probe a small upper surface layer of the disk. However, it could also be the situation that the CO is essentially measuring the entire column of a very small column density of gas inside of the some radius. If this is the

case, the profile wings could be measuring gas inside of the truncation radius, and the amount of mass would not be dynamically important, for example, in terms of effecting the migration of protoplanets. This scenario has its own caveat, because if disk locking is effective, then gas interior to corotation is expected to be sub-Keplerian, in near-rigid rotation (Shu *et al.* 1994; Ostriker & Shu 1995). Therefore, the maximum observed gas velocity will still correspond to the corotation radius.

High spectral resolution spectroscopy of the infrared transitions of CO provide a glimpse into disk gas at the inner edge of CTTS disks. At the same time, infrared interferometry has given us the first spatially resolved information on the hot dust continuum. We have begun to probe the disk truncation region of the star-disk interaction. Future refinement of the observations and analysis, and of the physical models for the interface of the disk and the magnetosphere, should enable us to better constrain and understand the physical processes centered in this region that are believed to be critical for star and planet formation.

References

Akeson, R. L. et al. 2005, *ApJ* 635, 1173
Cameron, A. C. & Campbell, C. G. 1993, *A&A* 274, 309
Carr, J. S., Tokunaga, A. T., Najita, J., Shu, F. H., Glassgold, A. E. 1993, *ApJ* 411, L37
Carr, J. S., Tokunaga, A. T., Najita, J. 2004, *ApJ* 603, 213
D'Alessio, P., Canto, J., Calvet, N., Lizano, S. 1998, *ApJ* 500, 411
Eisner, J. A., Hillenbrand, L. A., White, R. J., Akeson, R. L., Sargent, A. I. 2005, *ApJ* 623, 952
Königl, A. 1991, *ApJ* 370, L39
Kuchner, M. J. & Lecar, M. 2002, *ApJ* 574, L87
Lin, D. N. C., Bodenheimer, P., Richardson, D. C. 1996, *Nature* 380, 606
Muzerolle, J., Calvet, N., Hartmann, L., D'Alessio, P. 2003, *ApJ* 597, 149
Najita, J. R., Carr, J. S., Mathieu, R. D. 2003, *ApJ* 589, 931
Najita, J. R., Carr, J. S., Glassgold, A. E., Valenti, J. A. 2007, in: B. Reipurth, D. Jweitt & K. Keil (eds.), *Protoplanets and Planets V*, (Tucson: Univ. of Arizona), p. 507
Ostriker, E. & Shu, F. 1995, *ApJ* 447, 813
Romanova, M. M. & Lovelace, R. V. E. 2006, *ApJ* 645, L73
Salyk, C., Blake, G. A., Boogert, A. C. A., Brown, J. M. 2007, *ApJ* 655, 105
Simon, M., Dutrey, A., Guilloteau, S. 2000, *ApJ* 545, 1034
Shu, F., Najita, J., Ostriker, E., Wilkin, F., Ruden, S., Lizano, S. 1994, *ApJ* 429, 781